

11967

СООБЩЕНИЯ  
ОБЪЕДИНЕННОГО  
ИНСТИТУТА  
ЯДЕРНЫХ  
ИССЛЕДОВАНИЙ  
ДУБНА



С343а

I-98

19/III-79  
E4 - 11967

H.Iwe, H.J.Wiebicke

932/2-79

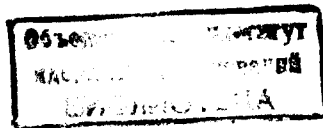
ON THE COULOMB POTENTIAL  
BETWEEN HEAVY IONS

**1978**

E4 - 11967

H.Iwe. H.J.Wiebicke\*

**ON THE COULOMB POTENTIAL  
BETWEEN HEAVY IONS**



---

\* Permanent address: Zentralinstitut für Kernforschung  
Rossendorf, DDR

Иве Х., Вибике Х.Я.

E4 - 11967

О кулоновском потенциале между тяжелыми ионами

В рамках обычного приближения удара получена простая аналитическая формула для кулоновского потенциала взаимодействия тяжелых ионов, которые рассматриваются как два однородно заряженных шарика. Это позволяет сделать некоторые оценки без численных расчетов. Показано различие в угловых распределениях упругого рассеяния, рассчитанных с предложенным кулоновским потенциалом и потенциалом, полученным в приближении точечного заряда. Рассмотрен ряд примеров.

Работа выполнена в Лаборатории теоретической физики ОИЯИ.

Сообщение Объединенного института ядерных исследований. Дубна 1978

Iwe H., Wiebicke H.J.

E4 - 11967

On the Coulomb Potential Between Heavy Ions

Within the framework of the usual sudden approximation a short analytical formula is derived for the Coulomb potential between heavy ions which are regarded as two homogeneously charged spheres. The simplicity of the formula allows discussion of the potential without numerical calculations and suggests some approximations and estimations. The effects on the elastic scattering angular distributions for this form of the Coulomb potential as opposed to the one resulting from the point charge approximation, are demonstrated and discussed for a series of examples.

The investigation has been performed at the Laboratory of Theoretical Physics, JINR.

Communication of the Joint Institute for Nuclear Research. Dubna 1978

## 1. INTRODUCTION

In any heavy-ion reaction the Coulomb interaction between the target nucleus and the colliding ion plays an essential role. Nearly all Coulomb subroutines in computer codes calculating nuclear reactions are based on the approximation where the impinging ion is assumed to be a point charge. This treatment does not adequately reflect the true state of affairs except for very light ions. In the region where the nuclei begin to penetrate each other, their finite dimensions cannot be neglected since the surface region is the most important one for heavy-ion reactions. Therefore, a more realistic treatment of the Coulomb potential has been performed to manifest effects due to the deviations from the point charge depending on the combination target-projectile. Recently some papers dealing with this problem<sup>/1-6/</sup> have been published. The formulae presented in refs.<sup>/3-6/</sup>, however, possess a complicated structure and can hardly be used for practical calculations.

The aim of our study is to provide a very simple analytical formula for the potential between two homogeneously charged spheres. This is done in Sec. 2 after making general considerations concerning the Coulomb potential in the framework of the optical model for heavy ions and the validity of the sudden approximation used. The structure of the new formula is investigated in detail. Its simplicity, in contrast with formulae of other authors, allows discussion of the potential without numerical calculations and suggests simple approximations and estimations.

In Sec. 3 we compare the present Coulomb potential both with the normal Coulomb expression obtained from the point charge approximation and with those calculated on the basis of more realistic charge distributions as reported in refs. /4, 5/. We also try to appraise the worth of the approximation using sharp cutoff charge distribution.

In Sec. 4 the effects on the elastic scattering angular distribution for this form of the improved Coulomb potential as opposed to the one resulting from the point charge approximation, are demonstrated and discussed for a series of examples. The deviations found on the contrary to the papers /3, 4/, are discussed in detail.

Finally Sec. 5 gives the summary and conclusions.

## 2. THE COULOMB POTENTIAL

Let us assume that the charge distribution  $\rho_1(\vec{r})$  generating the electrical field  $U(\vec{r})$  is placed at the origin of the coordinates. Then the Coulomb potential  $V_c(x)$  between  $\rho_1(\vec{r})$  and another charge distribution  $\rho_2(\vec{r})$  is defined as that work that must be done in order to carry  $\rho_2$  against the field  $U(\vec{r})$  from infinity to a position  $\vec{x}$ . In this process the energy connected with the displacement of two rigid charged clouds is

$$V_c(x) = \int_{\rho_2} d\tau \rho_2(\vec{r} - \vec{x}) U(\vec{r}). \quad (1)$$

Eq. (1) contains nothing regarding the amount of work needed to form the distributions or to shift some constituents of them. In the case when one of the clouds,  $\rho_1$ , has been deformed, an additional energy due to the change of the self-energy

$$V_c' = \int_{\rho_1} d\tau \rho_1(\vec{r}) U(\vec{r}) \quad (2)$$

must be taken into account. Thus, the last equation provides dynamical potentials whereas eq. (1) gives electrostatic ones. The first procedure for calculating the potential  $V_c(x)$  is consistent with the idea of the sudden approximation in which the charges move so fast that internal rearrangements of charged constituents can be disregarded. In any nuclear reaction both potential types come into effect /7/ where the static or dynamical portion can prevail more or less strongly. It is difficult to handle the last part because it depends essentially on the underlying model. In this case the charge densities should be time dependent, a behaviour which is not very well known.

We use the Coulomb potential in optical model calculations. As is well known the important region of reaction is the peripheral one where the two densities overlap very little and there is good reason to believe that a simple potential concept could be meaningful. This optical potential determines the wavefunction throughout all space. It is defined to generate the same wavefunction beyond the region of interaction between complex nuclei as the true many-body problem. However there are various ways of extrapolating into the interior (e.g., sudden approximation or adiabatic limit) and the associated wavefunction will have different meanings. This must be kept in mind when the wavefunctions are used for elastic scattering or in a DWBA calculation of some reaction. In the nuclear potential of the usual optical model, no dynamical effects are taken into account. Therefore, it is also unnecessary to include those in the Coulomb potential, i.e., to go beyond the framework of the sudden approximation.

In this paper the nuclear charge density of both colliding nuclei is assumed to be a homogeneous sharp cutoff distribution with spherical symmetry. In Sec. 3 we shall see how well this assumption works.

## 2.1. Point-Sphere Coulomb (PSC)-Potential

According to eq. (1) the Coulomb potential between a point charge and a homogeneously charged sphere with the radius  $R_c$  (point-sphere Coulomb potential) is

$$V_c^{\text{PSC}}(x) = B \begin{cases} \frac{1}{2}(3-x^2) & \text{if } x \leq 1 \\ 1/x & \text{if } x \geq 1 \end{cases} \quad (3)$$

$$B = Z_1 Z_2 e^2 / R_c, \quad x = r / R_c.$$

Here, the well-known formula has been rewritten by using the dimensionless coordinate,  $x$ , which will later be useful. The formula consists of two factors: the first one represents the Coulomb barrier  $B$  reached at  $x=1$ , the second one is a polynomial describing the radial dependence.

Formula (3) originally was derived for the Coulomb interaction of a light particle, such as a proton, with a nucleus where the point charge approximation is quite reasonable. Nevertheless, expression (3) has been often extended to heavy-ion reaction calculations and the sum of both Coulomb radii has been taken as the total Coulomb radius,  $R_c = R_1 + R_2$ . This implies a point charge interacting with a fictitious nucleus consisting of a target nucleus whose radius is increased by  $R_2$  (fig. 1d). This procedure does not reflect reality and, therefore, it is not a sensible approximation.

## 2.2. Sphere-Sphere Coulomb (SSC)-Potential

A more realistic description is obtained taking the Coulomb potential between two homogeneously charged rigid spheres, with radii  $R_1$  and  $R_2$  ( $R_1 \geq R_2$ ) respectively, which can penetrate one another (fig. 1b).

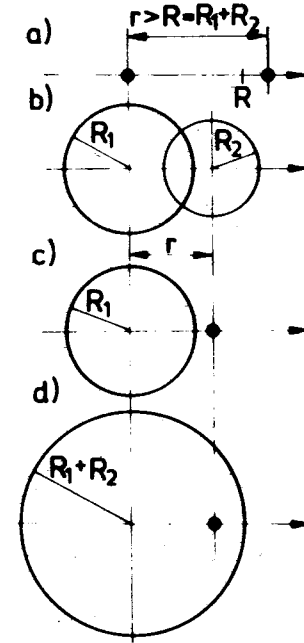


Fig. 1. Schematic pictures for determining the Coulomb potential between heavy ions: a) separated ions can be regarded as charged points, b) penetrating ions, c) the colliding ion is taken to be a charge point, d) usually used approximation for heavy ions.

Following eq. (1) we found a very simple analytical formula<sup>1/</sup> for this improved potential,

$$\frac{1}{2} b [3 - c - b^2 x^2] \quad x \leq x_0 \quad (4a)$$

$$V_c^{\text{SSC}}(x) = B \left\{ \frac{1}{x} \left[ 1 - 3d^2(1-x)^4 \left\{ 1 - \frac{2}{15}d(1-x)(5+x) \right\} \right] \right\} \quad \text{if } x_0 \leq x \leq 1 \quad (4b)$$

$$\frac{1}{x} \quad x \geq 1 \quad (4c)$$

$$a = R_1/R_2, \quad b = 1 + 1/a, \quad c = 3/(5a^2),$$

$$d = (a + 2 + 1/a)/4, \quad x_0 = (a-1)/(a+1).$$

For the same problem cumbersome and much more complicated expressions have been given in refs./<sup>3-6</sup>. However, after some manipulations our formula can be shown to agree with that first published by Donnelly et al./<sup>3</sup>, and also with those of refs./<sup>5,6</sup>. The transparent structure of formula (4) allows prediction of the effects of the potential without numerical calculations. This was achieved by the special choice of the dimensionless variable  $x = r/R_c = r/(R_1 + R_2)$  and by extracting the Coulomb barrier  $B = 1.4398 Z_1 Z_2 / (R_c \text{ in fm}) \text{ MeV}$ , which takes on the function of a scaling factor. The radial part describing the geometry of the problem depends only upon the ratio of the Coulomb radii  $a = R_1/R_2$ . A tabulation for different values of  $a$  is simple since realistic systems possess values within the small interval  $1 \leq a \leq 3$ , e.g.  ${}^7\text{Li}$  on  ${}^{197}\text{Au}$  ( $a = 3.04$ ),  ${}^6\text{Li}$  on:  ${}^{16}\text{O}$  ( $a = 1.39$ ),  ${}^{40}\text{Ca}$  ( $a = 1.88$ ) (these systems have been studied in/<sup>5</sup>) and  ${}^{16}\text{O}$  on:  ${}^{28}\text{Si}$  ( $a = 1.2$ ),  ${}^{40}\text{Ca}$  ( $a = 1.36$ ),  ${}^{128}\text{Sn}$  ( $a = 1.95$ ),  ${}^{208}\text{Pb}$  ( $a = 2.35$ ). Thus, the potential is separated into a geometry function and into a charge depending factor which is specific for a given system.

Now let us discuss the radial part in detail. In fig. 2 this function is represented for various values of  $a$  and is compared to the one for the PSC-potential. Outside the target nucleus ( $x \geq 1$ ) the well known term  $1/x$  in (3) and (4c) is obtained as though two point charges exist (fig. 1a).

In the overlapping region there is a strong difference between the SSC- and PSC-potentials which is maximal for symmetrical ion combinations ( $a = 1$ ). When the projectile is very much smaller than the target, formula (4) approaches the expression (3). The closer the contact of the ions is, the larger the difference becomes, reaching its maximum at  $x = 0$ . Here for  $a = 1$  the SSC-potential lies 60% higher than the PSC-potential (100%). For  $a = 2$  it is 42.5% higher and for  $a = 4$  it is still 23.5%.

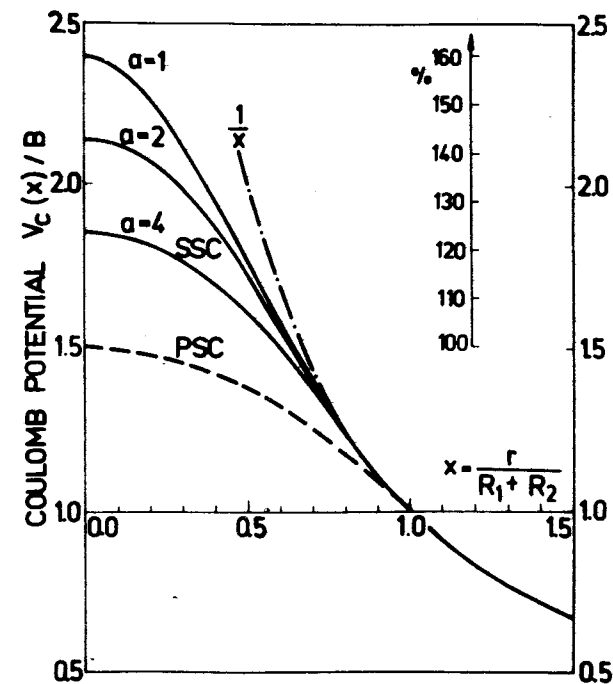


Fig. 2. Comparison of the SSC-potential for different ratios  $a = R_1/R_2$  (full lines) with the usual PSC-potential (dashed line). For illustration the curve  $1/x$  (dot-dashed line) is continued up to values  $x < 1$ . All potentials are reduced on their radial parts by extracting the Coulomb barrier  $B$ . Additionally a percentage scale is given.

Expressing the differences in energies one gets, for example, for  ${}^{16}\text{O}$  on  ${}^{16}\text{O}$  and  ${}^{16}\text{O}$  on  ${}^{208}\text{Pb}$  about 12.5 MeV and 48 MeV, respectively. The effect of this strong enhanced potential on the scattering is discussed in section 4.

The radial part of the potential (4b) in the partial overlap region consists of two terms. The first one shows the hyperbolic behaviour,  $1/x$ , as does the potential in the external region. The second term in the quadratic brackets describes the deviation from  $1/x$  which is zero at  $x = 1$  and increases very slowly (with fourth order of



unphysical Coulomb radius parameters. The new formula (4) has no this disadvantage. It needs no further approximations and can easily be included in any computer code.

### 3.2. Potentials Resulting from Realistic Nuclear Charge Distributions

For the calculations of the SSC-potential (4) a sharp cutoff distribution has been used. Assuming spherical symmetry, the most accurate Coulomb potential should be obtained by using some well-known realistic charge distributions. For light ions, either the Gaussian or harmonic well type comes into question and for heavier ions the Fermi type<sup>4, 5/</sup>. The potentials following from these charge distributions can be determined only numerically via eq. (1).

De Vries and Clover<sup>4/</sup> have used Fermi type distributions for the  $^{16}\text{O} + ^{208}\text{Pb}$  system and have pointed out that beyond  $x = 0.7$   $V_c^{\text{SSC}}$  differs from  $V_c^{\text{Fermi}}$  by less than 0.1% and at  $x=0$  by not more than 7%. Jain et al.<sup>5/</sup> have obtained an excellent overall correspondence for  $^{40}\text{Ca} + ^{40}\text{Ca}$  using the same charge distributions. For lighter ions  $^6\text{Li}$  and  $^{16}\text{O}$  they have assumed the Gaussian and harmonic well radial dependence, respectively, to calculate the potentials of the ion systems such as  $^{16}\text{O} + ^{16}\text{O}$ ,  $^{16}\text{O} + ^{40}\text{Ca}$ ,  $^6\text{Li} + ^{16}\text{O}$  and  $^6\text{Li} + ^{40}\text{Ca}$  which were found to be in good agreement with the SSC-potential for  $x \geq 0.3$ . For  $x < 0.3$  the authors got strong deviations and the curves calculated with realistic charge distributions enhance very rapidly if  $x \rightarrow 0$ . For  $^{16}\text{O} + ^{40}\text{Ca}$ , at  $x = 0.1$  the curve reaches a value  $> 200 \text{ MeV}$  (fig. 4 in ref.<sup>5/</sup>), much more than for  $^{40}\text{Ca} + ^{40}\text{Ca}$  in the same picture. As is shown by the following argument this strong increase is not understandable. The maximum amount of work in the electrical field of a target nucleus with a fixed charge distribution must be done if the colliding ion is regarded as a point charge and is shifted to the centre,  $x=0$ . That must be the upper limit for all

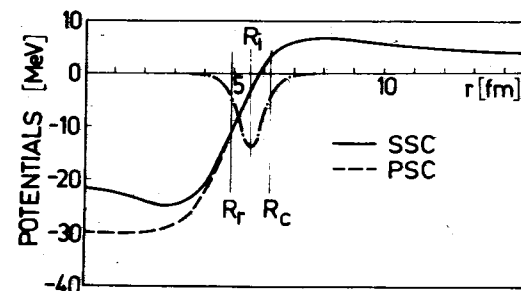


Fig. 4. Real and imaginary (dash-dotted) part of the optical potential for the reaction  $^{11}\text{B} + ^{16}\text{O}$ .

charge distributions of the lighter ion. This value amounts to about 80 MeV for  $^{40}\text{Ca} + ^{40}\text{Ca}$ .

On the other hand the region  $x \leq 0.3$  is not important in heavy ion elastic scattering potentials because the absorption prevents a strong penetration of the nuclei<sup>8/</sup>.

The examples investigated in refs.<sup>4, 5/</sup> are representative for all other target-projectile combinations of light and intermediate nuclei. They show that realistic charge distributions, compared to the sharp cutoff potential, bring about small effects in the resulting potential for core-core separations  $x > 0.3$ . These small effects cannot justify the use of computer-time-consuming realistic charge distributions.

### 4. EFFECTS OF THE SSC-POTENTIAL ON ANGULAR DISTRIBUTIONS

For illustrating the influence of the improved Coulomb potential  $V_c^{\text{SSC}}$ , we have tested the effect of using  $V_c^{\text{SSC}}$ , versus  $V_c^{\text{PSC}}$  on elastic scattering in the framework of the optical model. Decisively, the amount of the effect depends on the combination of target-projectile in a twofold way: on the geometry and on the mass region of the colliding ions used. As was mentioned above and was found also by Jain et al.<sup>5/</sup>, the largest effect can be expected for nuclei with the same or nearly the

same radii  $R_1 \approx R_2$  ( $a \approx 1$ ), i.e., for symmetrical systems. The reason for the dependence on the mass region lies in the competition between the Coulomb potential and the nuclear potential. In the following this will be investigated for three groups:

i) light nuclei: the Coulomb potential contribution of 30% is relatively small compared to the nuclear potential. Therefore, a choice of the Coulomb constant  $R_c$  is not critical.

ii) intermediate nuclei: the Coulomb and nuclear potential are of the same order of magnitude and can bring strong interference structures. The Coulomb radius  $R_c$  becomes a critical quantity.

iii) heavy nuclei: the Coulomb potential dominates whereas the nuclear potential appears only as a correction.

The SSC-potential lies higher than the PSC-potential. The difference grows monotonically towards the internal region. The effective potential (the sum of all real parts of the optical potential) is thereby raised. The influence of the SSC-potential on the effective potential depends on the potential type taken into account. It becomes larger if the nuclear potential is of a shallow type and smaller for a deep type. Whether this difference will come into effect or not depends on the absorption of the optical potential. A large absorption hinders the propagation of waves to the centre. On the other hand a small or  $\ell$ -depending absorption<sup>18/</sup> allows the waves to come in and to feel the difference. In dependence on optical parameters, a part of the absorption may be reduced for growing angular momenta  $\ell$  so that the effective absorption is diminished to the  $\ell = 0$  limit. This behaviour can bring about  $\ell$ -staggering whereby some partial waves are favoured and determine the shape of the angular distribution. This  $\ell$ -staggering is influenced by the change of the PSC- to the SSC-potential and modifies the angular distribution in a special way. A new fitting procedure is necessary to provide another best-fit optical parameter set. However a search for new parameters lies outside the scope of this paper.

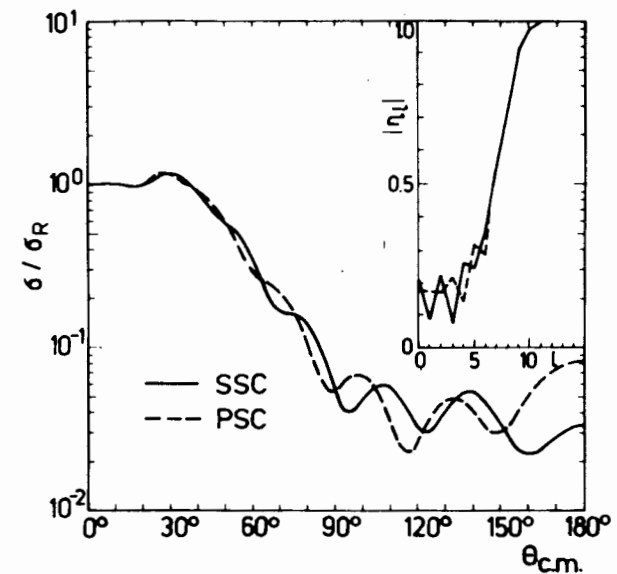


Fig. 5. Reflection coefficients and angular distributions of the elastic scattering of  $^{11}\text{B}$  on  $^{16}\text{O}$  at  $E_{\text{lab}}=27 \text{ MeV}$  calculated on the basis of the SSC- and PSC-potentials.

#### 4.1. Light Nuclei

Reaction  $^{11}\text{B} + ^{16}\text{O}$ :

For the elastic scattering of  $^{16}\text{O}$  on  $^{11}\text{B}$  at  $E_{\text{lab}} = 27 \text{ MeV}$  in ref. <sup>19/</sup> a best-fit optical parameter set was found which contains a large Coulomb radius parameter of  $r_{oc} = 1.45 \text{ fm}$  compared to that one of the surface absorption of  $r_{os} = 1.1 \text{ fm}$ . Fig. 4 shows the strong difference of the effective potentials incorporating the PSC- and SSC-potentials which, for example, at  $r = 3.5 \text{ fm}$  ( $x = 0.6$ ) is already  $3 \text{ MeV}$ . The resulting reflection coefficients (insert in fig. 5) show for the PSC-potential a distinctly marked staggering. The SSC-potential does not change the staggering at large  $\ell$ , however, the maxima and minima are completely out of

phase. This behaviour causes that the angular distributions resulting from the SSC- and PSC-potential oscillate with shifted phases to each other (fig. 5).

Reaction  $^{16}\text{O} + ^{18}\text{O}$ :

The optical potential used in ref.<sup>/10/</sup> for this elastic scattering reaction contains an  $\ell$ -dependent volume absorption. As can be seen in fig. 6 the angular distributions for this reaction corroborate the above discussion.

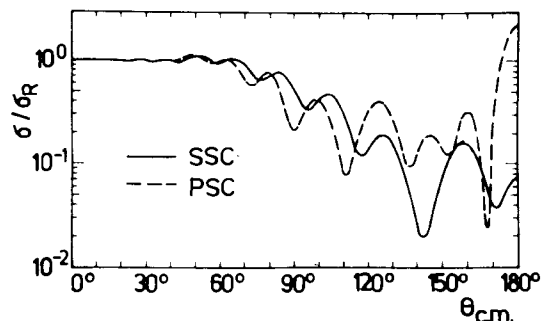


Fig. 6. Angular distribution for the elastic scattering of  $^{16}\text{O}$  on  $^{18}\text{O}$  at  $E_{\text{lab}} = 24 \text{ MeV}$ . The optical potential parameters are taken from ref.<sup>/10/</sup>. The dashed curve agrees with that one given in fig. 3 of this reference.

#### 4.2. Intermediate Nuclei

Reaction  $^{28}\text{Si} + ^{29}\text{Si}$ :

The optical potential for the elastic scattering of  $^{28}\text{Si}$  on  $^{28}\text{Si}$ <sup>/10/</sup> also possesses an  $\ell$ -dependent volume absorption and belongs to the family of deep potentials. In the region  $5 < r < R = 7.4 \text{ fm}$  ( $0.7 < x < 1$ ) large deviations exist (e.g.,  $5 \text{ MeV}$  at  $x = 0.7$ ) between the effective potentials resulting from the SSC- and PSC-potentials (fig. 7). For  $r < 5 \text{ fm}$  the SSC-potential is strongly enhanced versus the PSC-potential. The reflection coeffi-

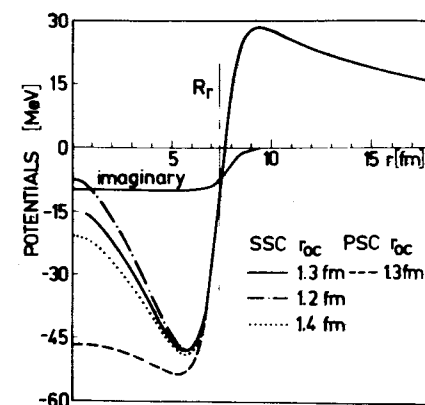


Fig. 7. Real and imaginary part of the optical potential for the reaction  $^{28}\text{Si} + ^{29}\text{Si}$ .

icients (insert in fig. 8) of the SSC-potential show an excessive damping of the  $\ell$ -staggering in comparison with those of the PSC-potential but the positions of the maxima and minima are unchanged. The differences in the angular distributions, particularly in the backward angles, can be seen in fig. 8.

A variation of the Coulomb radii in the SSC-potential leads to the angular distributions shown in fig. 9. The curve belonging to  $r_{\text{oc}} = 1.2 \text{ fm}$  lies visibly under that of  $r_{\text{oc}} = 1.4 \text{ fm}$ , and both are completely out of phase with each other. This behaviour can be understood in terms of the reflection coefficients (insert in fig. 9). For  $r_{\text{oc}} = 1.4, 1.3, 1.2 \text{ fm}$  a monotonic damping of the staggering is found. The staggering curve of  $r_{\text{oc}} = 1.2 \text{ fm}$  is shifted by one unit to the right relative to the curve of  $r_{\text{oc}} = 1.4 \text{ fm}$  so that the maxima correspond to the minima of the other curve.

#### 4.3. Heavy Nuclei

As stated above, the Coulomb potential of nuclei belonging to the mass region concerned dominates in the effective potential. The latter is only repulsive and

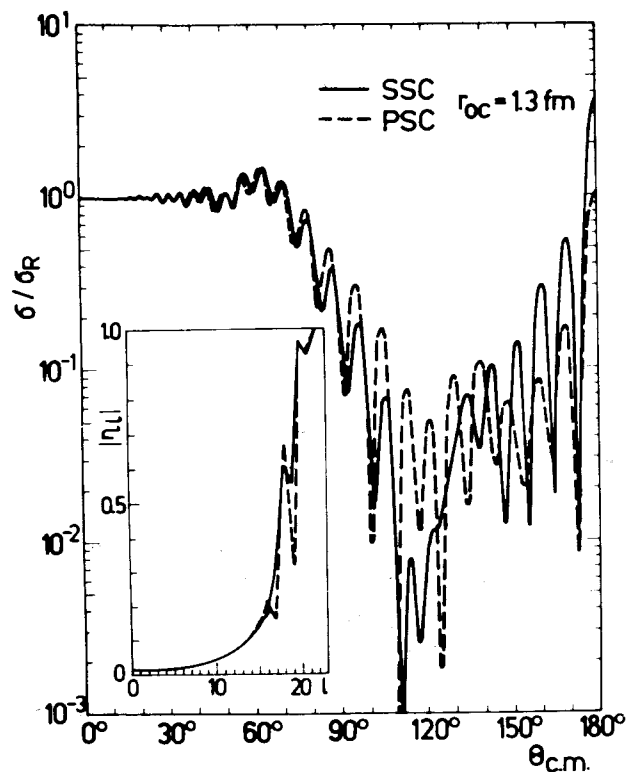


Fig. 8. Reflection coefficients and angular distributions of the elastic scattering of  $^{28}\text{Si}$  on  $^{29}\text{Si}$  at  $E_{\text{lab}} = 70$  MeV calculated on the basis of the SSC- and PSC-potential. The dashed curve agrees with that one given in fig. 12 of ref. <sup>10/</sup>.

hinders the waves to enter the interior so that the difference of both potentials cannot be felt by them. Therefore, no effect can be expected in the angular distribution of the elastic scattering. For this reason no pictures are given by us. De Vries and Clover <sup>4/</sup> have chosen the reaction  $^{16}\text{O} + ^{208}\text{Pb}$  for their study of the SSC-potential. In comparison to the PSC-potential they have not got any deviations and, thus, confirm the above considerations.

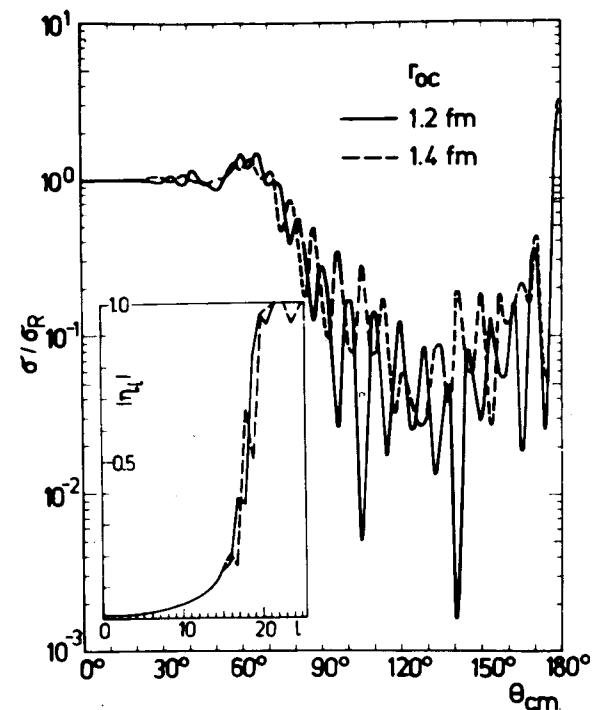


Fig. 9. The same as in fig. 8 but for different Coulomb radii.

## 5. SUMMARY AND CONCLUSIONS

Within the framework of the sudden approximation a simple formula for the Coulomb potential of two homogeneous charge distributions was found. By introducing a dimensionless coordinate  $x = r/(R_1 + R_2)$  and the ratio  $a = R_1/R_2$ , a separation into a charge dependent factor and a radial function describing the geometry of the problem was managed. The factor is identical with the Coulomb barrier  $B$  and the radial function depends on the only parameter  $a$ . Thus, this formula is well suitable to make simple estimations of the Coulomb potential. The comparison of the SSC- and PSC-potentials

shows a strong difference in the radial dependence. It is equivalent to a considerable alteration of the Coulomb radius expressed by a reduction factor. Contrary to the conclusions of the authors of refs.<sup>3, 4</sup> we found realistic examples where the finite dimension of the nuclear charge distribution has a substantial influence on the angular distribution of the elastic scattering. These differences are shown to be the largest for nuclei of the intermediate mass region. The effect of the SSC-potential essentially depends on the absorption and is most large for small absorptions appearing in a shallow potential or  $l$ -depending absorption model. The homogeneous charge distribution can be regarded as an excellent approximation to realistic nuclear charge distributions. Therefore there is no reason to use computer-time-consuming numerical procedures for calculating the potential starting from special realistic charge distributions. The analytical shape of the derived formula is so simple that it can easily be inserted in any computer code.

#### REFERENCES

1. Iwe H., Wiebicke H.-J. *ZfK-297*, 1975.
2. Krappe H.-J. *Ann. of Phys.*, 1976, 99, p.142.
3. Donnelly T.W., Dubach J., Walecks J.D. *Nucl. Phys.*, 1974, A232, p.355.
4. DeVries R.M., Clover M.R. *Nucl. Phys.*, 1975, A243, p.528.
5. Jain A.K., Gupta M.C., Shastry C.S. *Phys. Rev.*, 1975, C12, p.801.
6. Poling J.E., Norbeck E., Carlson R.R. *Phys. Rev.*, 1976, C13, p.648.
7. Park J.Y., Scheid W., Greiner W. *Phys. Rev.*, 1974, C10, p.967.
8. Moffa P.J., Dover C.B., Vary J.P. *Phys. Rev.*, 1976, C13, p.147.
9. Delic G. *Phys. Lett.*, 1974, 49B, p.412.
10. Gelbke C.K., Bock R., Richter A. *Phys. Rev.*, 1974, C9, p.852.

Received by Publishing Department  
on October 20 1978.